FAST PARTICLE DRIVEN ALFVÉN EIGENMODES IN TOKAMAKS

S.E. Sharapov

Euratom/CCFE Fusion Association, Culham Science Centre, Abingdon OX14 3DB, UK

ABSTRACT

Instabilities of Alfvén Eigenmodes (AEs) are often excited by a super-Alfvénic population of fast ions accelerated with ion cyclotron resonance heating (ICRH) or produced by neutral beam injection (NBI) in present-day tokamaks. In view of the next-step burning plasma experiments with super-Alfvénic alpha-particles, the experimental data on AE instabilities is reviewed for large volume JET tokamak, high magnetic field C-MOD tokamak, and high-beta START and MAST tokamaks. The main types of AE instabilities are described and compared to theory.

I Introduction

The tokamak reactor concept is based on the idea that, once ignited, the deuterium-tritium (DT) plasma in a tokamak becomes self heated through alpha-particles born in fusion D-T reactions with birth energy 3.5 MeV [1]. The alpha-particle production, heating, transport, and losses must be understood well enough to predict with certainty the alpha-particle behaviour in a fusion reactor. Continued investigations of Alfvén Eigenmodes (AEs) in tokamaks are motivated by the potential of such waves to affect significantly transport of alpha-particles via wave-particle resonant interaction between AEs and population of alpha-particles since for typical plasma parameters the following ordering is valid [2]:

$$V_{Ti} << V_A \le V_f << V_{Te}, \qquad (1)$$

where $V_f \equiv V_{fast}$ is the fast ion (alpha particle) averaged velocity, V_{Ti}, V_{Te} are thermal velocities of the bulk ions and electrons, and $V_A = B_0 / \left(4\pi \sum_i n_i m_i \right)^{1/2}$ is the Alfven velocity, B_0 is the equilibrium magnetic field and n_i, m_i are the density and the mass of the bulk plasma ions. The condition (1) tells us that AE, which is a weakly-damped type of shear Alfvén wave in toroidal geometry, can satisfy the resonance condition $V_{\|f} = V_A$ between AE and alpha particles during their slowing-down, while the phase velocity of AEs is far away from the resonances with thermal ions and electrons.

The resonant interaction between alpha-particles and AEs can release a free energy source associated with radial gradient of the alpha-particles [3,4] if the alpha-particle pressure becomes large enough to overcome the total AE damping by the bulk plasma,

$$\frac{\gamma_f}{\omega_{AE}} = -\left(1 - \frac{\omega_{*f}}{\omega_{AE}} \right) \cdot F\left(\frac{V_f}{V_A} \right) \ge \frac{\left| \gamma_i + \gamma_e \right|}{\omega_{AE}}. \qquad (2)$$

Here, γ_f is the growth rate of AE caused by the fast ions, $\omega_{*f} = -k_\vartheta \left(V_f^2 / \omega_{C\,f} \right) \left(1/p_f \right) dp_f / dr$ is the fast ion drift frequency [3], ω_{AE} is the frequency of the mode considered, $F\left(V_f / V_A \right)$ is a function that depends on the distribution function of the fast ions in velocity space, γ_i, γ_e are the damping rates of AE associated with bulk ions and electrons, $\omega_{C\,f}$ is fast ion cyclotron frequency, p_f is fast ion pressure, and k_ϑ is poloidal wave vector of AE. If the condition (2) is satisfied, the amplitude of the AE increases and the AE of high amplitude may eject energetic alpha-particles from the core of a fusion reactor, possibly leading to a significant reduction in the alpha heating efficiency and to the damage of the tokamak first wall.

In present day tokamaks, instabilities of AEs are excited by super-Alfvénic fast ions accelerated with ion cyclotron resonance heating (ICRH) or produced by neutral beam injection (NBI). Experimentally, AEs are seen most often as discrete frequency toroidal Alfvén eigenmodes (TAEs) [5]; discrete frequency Alfvén cascade (AC) eigenmodes [6,7] in plasmas with reversed magnetic shear, and energetic particle modes (EPMs) [8] whose frequencies sweep in time faster than the equilibrium parameters change. Under certain conditions the unstable AEs can cause significant loss of beam ions, e.g. up to 50% of input NBI power in some DIII-D experiments [9].

For reviewing existing experimental data and for identifying the key elements of AE instabilities, it is useful to consider the following main avenues for studying AEs:

- Type of the tokamak and specific properties of plasma in this particular type of the machine;
- AE spectrum in the equilibrium considered (number and type of AEs, linear drive and damping effects);
- Type of the near-threshold nonlinear evolution of unstable AE (soft or hard nonlinear regimes).

Section II of this paper describes main types of tokamaks, Section III presents experimental data and brief theoretical description of AEs, Section IV discusses nonlinear AE evolution, and Section V presents summary.

II Three main tokamak concepts

The development of nuclear fusion in magnetically confined plasmas has a major milestone in the form of the triple-product ignition criterion [1], $nT\tau > 5\times10^{21}$ m^{-3} keV·s (~ 10 atm·s), valid for deuterium-tritium plasmas with fusion-grade temperature T ~ 10-20 keV with plasma density n and plasma energy confinement time τ. This criterion can be expressed through engineering parameters of a magnetic fusion device,

$$\beta \cdot \tau \cdot B_0^2 > 4 \text{ T}^2 \cdot \text{s}, \qquad (3)$$

where $\beta \equiv \left(8\pi / VB_0^2\right) \int pdV$ is the ratio of the plasma pressure $p = nT$ to the pressure of the confining vacuum magnetic field in the plasma volume V. The criterion (3) shows that there are three main ways to achieve ignited DT fusion in a magnetic system [10]:

1) Increasing τ. In effect this leads to fusion reactors with larger volume since for a steady-state fusion reactor with alpha-particle heating power P_α thermal plasma energy $W = 2k_B nTV$ satisfies

$$\frac{dW}{dt} = 0 = P_\alpha - \frac{W}{\tau}, \qquad (4)$$

so that $P_\alpha = W/\tau = 2k_B nT\left(V/\tau\right)$, where k_B is Boltzman constant. It follows from (3), (4) that for a given power of fusion reactor, say ~ 1GW, and for typical tokamak parameters $B_0 = 5$T, $\beta \approx 4\%$, a critical ignition volume of $V_{crit} \approx 1000$ m^3 must be used for achieving the ignition via increasing τ. This approach of building larger machines is dominating tokamak development, with Joint European Torus (JET) [11] being the largest machine with volume 100 m^3. This approach is adopted for the ITER device [2].
2) Increasing the magnetic field strength. For this to be realised one has to use magnetic fields exceeding 5 T, which is quite high already. The approach of achieving fusion along this avenue is approached in present day machine C-MOD (see, e.g. [12] and Refs. therein), and is adopted in the Italian design IGNITOR [13] and in the US design FIRE [14].
3) Increasing β. In contrast to the two options above, which have technological difficulties of obtaining either larger volume or higher field, the problem of increasing β has to deal with the "laws of nature" as β is limited by MHD instabilities of the plasma. A level of a few percent β is typical for conventional tokamaks, and the way to achieve higher β-values may be approached by optimising the magnetic field topology beyond the conventional approach. The spherical tokamak (ST) concept [15] is one of the promising developments since $\beta \approx 40\%$ were demonstrated on START [16], with the central values $\beta(0) \cong 1$. Burning plasma machines, e.g. Spherical Tokamak Power Plant (STPP) [17] are being discussed for the ST concept.

Up to now, fusion has been concentrating on approaching the criterion (3) in a sub-critical mode. No self-burning plasma effects were explored in majority of plasmas so far, and weak self-burn was investigated in the TFTR and JET DT campaigns. For preparing the next-step burning plasma experiments, some key problems should be investigated, such as whether alpha particle pressure will behave like that of thermal plasma with respect to plasma stability involving critical pressure limits, and whether burning plasmas will self-excite AEs resulting in re-distribution and losses of alpha-particles. Experiments on present-day tokamaks can answer some of these questions by producing significant populations of fast ions mimicking alpha-particles in terms of $V_f / V_A \geq 1$ and $\omega_{*f} / \omega_{AE} > 1$ necessary for AE instabilities. Next two sections describe such experiments.

III Spectrum of Alfvén Eigenmodes: theory and experiment

In cylindrical or toroidal inhomogeneous plasmas, shear Alfvén waves [1] with a dispersion relation

$$\omega_A\left(r\right) = \pm k_\parallel\left(r\right) \cdot V_A\left(r\right), \qquad (5)$$

form a continuum and may also form a discrete spectrum of eigenmodes if an extremum of Alfvén continuum exists at some radial points $r = r_0$ (see, e.g. [7] and References therein):

$$\left(d\omega_A\left(r\right)/dr\right)\Big|_{r=r_0} = 0. \qquad (6)$$

Here, $k_\parallel \equiv \mathbf{k} \cdot \mathbf{B}_0 / B_0$ is the parallel wave-vector of Alfvén wave. One can interpret the formation of discrete eigenmodes as follows. In the vicinity of an extremum point (6), perpendicular refraction index of electromagnetic wave, $N_r = \left(ck_r / \omega_A\right)$, has an extremum, and the inhomogeneous plasma forms a waveguide similar to fiber optics at $r = r_0$ with a radially localised Alfvén eigenmode (AE) in it. This AE has a discrete eigenfrequency

$$\omega_{AE} = \omega_A\left(r_0\right) + \delta\omega, \qquad (7)$$

that deviates from the Alfvén continuum (5) by $\delta\omega$, and if $\delta\omega$ exceeds the natural width of the AE eigenfrequency caused by the damping effects, $\left|\delta\omega\right| > \left|\gamma_i + \gamma_e\right|$, the AE eigenfrequency is well separated from (5) and no heavy continuum damping suppresses such a shear Alfvén wave.

In toroidal geometry, the extremum points (6) occur in toroidicity-induced gaps existing due to the toroidal coupling of poloidal harmonics as Figure 1 shows. A discrete Toroidicity-induced Alfvén Eigenmode (TAE) [5] exists in this case, due to a finite value of the magnetic shear S, $\delta\omega/\omega_A \propto S^2$, with TAE frequency within the TAE gap, $\omega_A^{\min}(r_0) < \omega_{TAE} < \omega_A^{\max}(r_0)$, so that TAE does not experience strong continuum damping.

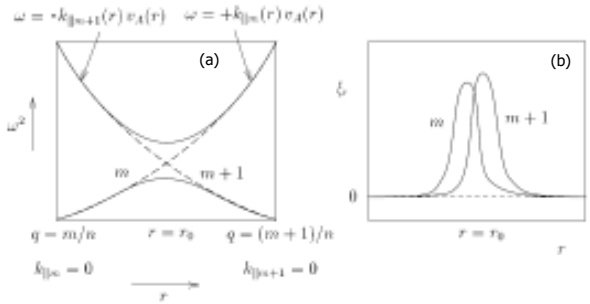

Fig. 1 (a) Alfvén frequency continuum in a torus showing coupled poloidal harmonics and (b) the corresponding TAE eigenfunction.

In addition to TAE, Alfvén eigenmodes may exist caused by an elliptical cross-section of the plasma (Ellipticity-induced AE, EAE), triangular cross-section of the plasma (Noncircularity-induced AE, NAE), and modes associated with reversed magnetic shear (Alfvén cascade eigenmodes, AC [6,7]). TAE, EAE, and NAE have quite similar physics and differ mostly in frequency, $\omega_{TAE} \approx V_A/(2qR_0) \approx \omega_{EAE}/2 \approx \omega_{NAE}/3$. Alfvén cascade eigenmodes are not caused by coupling of poloidal harmonics, in contrast to TAE, EAE, and NAE, and we look at AC versus TAE now.

III.1 Experimental observations of AEs on JET

For considering experimental data on AEs, we first focus on the largest volume present day machine JET. On JET with typical magnetic field 3.4 T, fast ions produced by NBI with injection energy 80-140 keV are sub-Alfvénic and cannot be used for studying TAE instabilities. However, super-Alfvénic population of fast ions can be produced on JET with ion cyclotron resonance heating (ICRH). The ICRH-accelerated ions have perpendicular velocity much higher then parallel one so orbits of these ions are trapped, and the value of $V_{\|f}$ varies along the ion orbit. There is no wave-particle resonance $V_{\|f} = V_A$ in this case. Instead, the trapped particle resonance condition satisfies

$$\omega_{AE} = l \cdot \omega_{fb} + n \cdot \omega_{fD}, \qquad (8)$$

where ω_{fb}, ω_{fD} are trapped particle poloidal and toroidal orbit frequencies [1], n is the AE toroidal mode number, and l is an integer value. Although the efficiency of ICRH drive differs from the efficiency of the drive for fusion-born alpha-particles, the AE spectrum itself can be investigated in JET experiments with ICRH.

Here, we consider AEs in JET discharges with increasing inductive currents and power waveforms shown in Fig.2 [7]. The only difference between the discharges is that low-power Lower Hybrid Ccurrent Drive, $P_{LHCD} \approx 2.5$ MW, is applied in discharge #49382. This LHCD applied early in the discharge creates a non-monotonic profile of the safety factor $q(r) \approx rB_T/RB_P$ with a region of reversed magnetic shear), while in the comparison discharge (#49384) the $q(r)$-profile is monotonic.

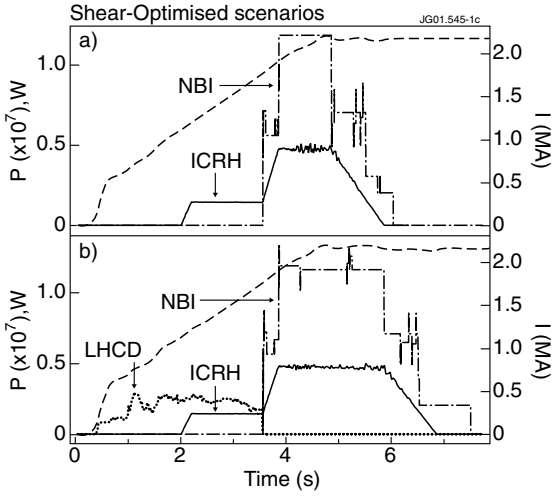

Fig. 2 Two similar JET discharges (pulses #49384 (a) and #49382 (b) with toroidal magnetic field $B_T = 2.6$ T and plasma current $I_P^{\max} = 2.2$ MA) with the only difference in 2.5 MW of LHCD applied at the pre-heating phase in #49382. In both discharges current shown by broken line was increasing from $I_P = 1.1$ MA at $t = 2$ s to $I_P = 2.2$ MA at $t = 5$ s.

The measurements of AEs are performed on JET using a toroidal set of high-resolution magnetic pick-up coils located just outside the plasma and connected to an analog to digital converter with a sampling rate of 1MHz [18]. Magnetic fluctuation data, $\partial(\delta B_p)/\partial t$, caused by AEs are recorded with 12 bit resolution. This measurement allows determination of the mode amplitude at the edge to an accuracy $|\delta B_p/B_0| \le 10^{-8}$. In addition, a toroidal set of three coils allows determination of the toroidal mode numbers from the relative phase of the AEs from *n* =-17 to *n* =17. Figs. 3(a) and (b) show magnetic fluctuation data measured by the magnetic pick-up coils in the Alfvén frequency range during the pre-heating phase of two discharges with the power and current wave-forms shown in Fig.2.

A comparison of Figs 3(a) and (b) reveals that the Alfvén instabilities are very different in the two discharges. In the plasmas with a monotonic $q(r)$-profile (#49384) the ICRH-accelerated hydrogen minority ions excited TAEs, whose frequency followed the increase of plasma current in time.

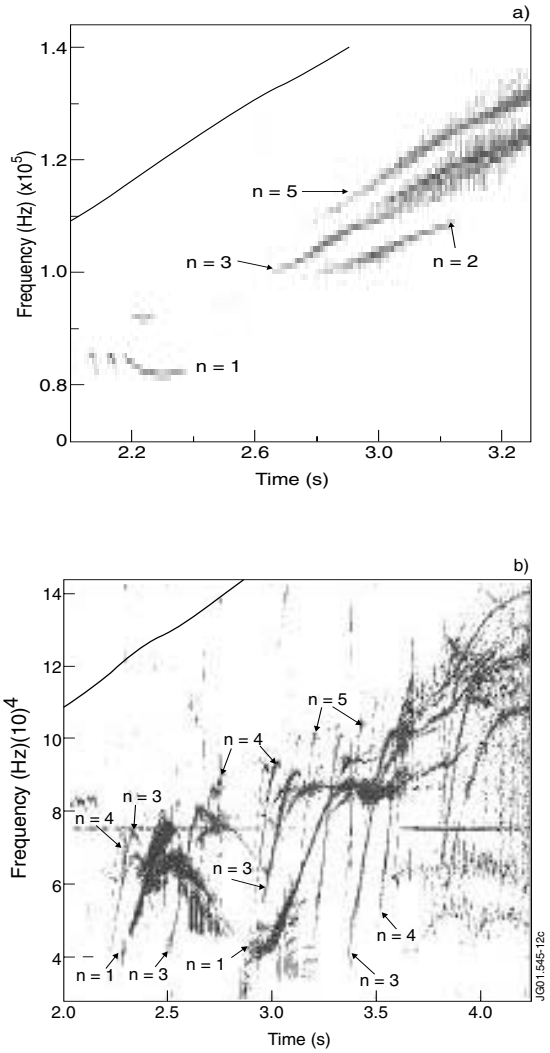

Fig.3 (a) Spectrogram of the magnetic perturbations in plasma with monotonic $q(r)$. TAE modes are observed at frequencies $f_{TAE} \cong$ 80-200 kHz. Evolution of TAE-frequency in time is caused by plasma current increase at the time of observation (the trace shows the slope of the current increase). (b) Spectrogram of the magnetic perturbations in plasma with non-monotonic $q(r)$. Alfvén cascades are observed at frequencies below TAE frequency range, $f_{AC} \cong$ 40-90 kHz << f_{TAE}. Multiple branches of Alfvén cascades ranging from n=1 to n=6 are observed, with frequency sweeping proportional to the mode number. The trace shows the slope of the plasma current increase.

The comparison discharge, in which LHCD created a non-monotonic $q(r)$-profile, exhibits Alfvén cascade (ACs) eigenmodes with the frequency sweeping below the TAE frequency, shown in Fig.3(b). Each AC in Fig.3(b) has pronounced upward frequency sweeping with rate proportional to the toroidal mode number n and faster than the current increase rate. During the AC evolution, the frequency increases up to the frequency of the TAE-gap, and AC either transforms into a TAE or disappears. Internal measurements of AC eigenmodes with the ECE and SXR diagnostics in JET reversed-shear discharges with high ICRH power, have shown that AC eifenmodes are localised in the vicinity of zero shear region.

The difference between TAE and AC has been explained as follows. The extremum condition (6) is satisfied for TAE due to toroidal coupling of two poloidal harmonics independently of the type of the safety factor. If a non-monotonic profile of the safety factor $q(r)$ is obtained in the discharge, an additional extremum point r_0 associated with the minimum value of $q(r)$, $q_{\min}$, appears at which (6) is satisfied. An eigenmode, which consists of a single poloidal harmonic, can be formed then in vicinity of r_0 due to the effect of fast ions [6,7] or equilibrium effects of $\varepsilon^2 \approx \left(r^2/q\right)\cdot\left(d^2q/dr^2\right)$ [19] in a weakly reversed shear case.

Due to the increase in the inductive current, $q_{\min}(t)$ value decreases in time, and the frequency of Alfvén continuum (5) at r_0 becomes a function of time, too

$$\omega_A(r_0,\ t) = \frac{V_A}{R_0}\left|n - \frac{m}{q_{\min}(t)}\right|. \qquad (9)$$

Due to this time dependence, Alfvén continuum undergoes tranformations shown in Figure 4. The frequency associated with the "tip" of the Alfvén continuum at r_0 behaves then as the traces of $\omega_A(r_0,t)$ show in Figure 5. It is seen that the tips of the Alfvén continua with $n = 1,\ 2,\ 3$ determined by equation (9), exhibit in toroidal geometry a pattern similar to the experimentally observed in Figure 3(b). Namely, the rate of the frequency sweep is proportional to the toroidal mode number, modes with different toroidal mode numbers have different periodicity in time, and there exists certain time when the tips of the Alfvén continua with different toroidal mode numbers all together start to grow from zero frequency. These times correspond to times of integer $q_{\min}$ values, and this set of ACs occuring simultaneously is called Alfvén Grand Cascade [7].

Typical saturation amplitudes of AEs driven by ICRH-accelerated fast ions on JET, are quite low and do not cause notable re-distribution of fast ions, apart from some discharges with tornado modes in sawtoothing plasmas [20]. Under these conditions, the observation of numerous and harmless AEs can become beneficial as these allow one to obtain important information on plasma equilibrium properties [7, 21]. This technique of MHD spectroscopy is best used for diagnosing the temporal evolution of $q_{\min}$ and associated phenomena of triggering internal transport barriers [22].

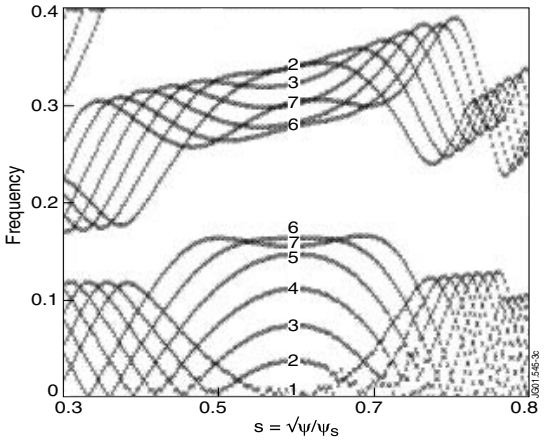

Fig.4 The ideal MHD CSCAS code [23] showing normalized frequency $\omega R_0 / V_A(0)$ of $n = 1$ Alfvén continuous spectrum as a function of radius $s = \left(\psi_P / \psi_P^{edge}\right)^{1/2}$ for several values $q_{\min}$ during the evolution of $q_{\min}(t)$ from $q_{\min}$ = 3 down to $q_{\min}$ = 2.4 in reversed shear JET discharge. The sequence of Alfvén continuum tips corresponding to values $q_{\min}$ =3, 2.9, 2.8,…, 2.4 is shown by numbers 1,…,7.

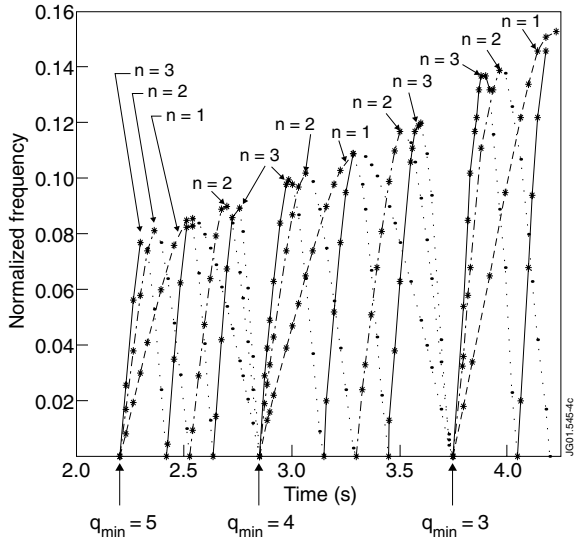

Fig.5. The CSCAS analysis showing temporal evolution of the normalised frequency $\omega_A(r_{\min})R_0 / V_A$ at $q = q_{\min}$ as $q_{\min}(t)$ decreases in time. Mode numbers plotted are $n = 1$, $n = 2$ and $n = 3$. Solid lines indicate times of local maximum of the Alfvén continuum, while broken lines indicate times of local minimum of the Alfvén continuum.

III.2 Experimental observations of AEs on C-MOD

Alfvén Eigenmodes driven by ICRH-accelerated ions are often observed in plasmas of C-MOD tokamak with high magnetic field [12]. Both TAE and AC eigenmodes are typical of these plasmas. Apart from the higher frequency of the modes caused by higher magnetic field, and somewhat different parameters of fast ion distribution function caused by denser plasma, the phenomenology of AEs on C-MOD is quite similar to JET observations described above.

III.3 Experimental observations of AEs in ST plasmas

Experimental data on AE instabilities observed in plasmas of spherical tokamaks, e.g. START [16] and MAST [23] differs from that on JET. Due to the low value of magnetic field, $B_0 \leq$ 0.5 T, on these present-day STs, the value of Alfvén speed is much lower than that on JET or C-MOD, so that beam ions produced with NBI of relatively low energy, 30-60 keV, satisfy the fundamental $V_{\|f} = V_A$ resonance between the beam ion velocity and AE mode. This type of resonance is similar to the one expected for fusion-born super-Alfvénic alpha-particles, so that STs can be considered as test-beds for Alfvén wave physics.

On both the START (major radius $R_0 \approx 0.3 \div 0.37$ m; minor radius $a \approx 0.23 \div 0.3$ m; $I_P \approx 300$ kA; $B_0 \approx 0.15 \div 0.6$ T) and MAST ($R_0 \approx 0.9$ m; $a \approx 0.7$ m; $I_P \approx 1.35$ MA; $B_0 \approx 0.4 \div 0.7$ T) hydrogen or deuterium NBI into deuterium plasmas was used, with the centre of the neutral beam line approximately tangential to the magnetic axis. The maximum beam energy was 30 keV with maximum input power about 1 MW on START and 45 keV and 3.2 MW in MAST experiments reported here. In both STs, plasmas with density comparable to that of large-size conventional tokamaks are usually obtained at magnetic fields which are about an order of magnitude lower than those in the conventional machines. This implies that plasmas in START and MAST have a very low Alfvén speed, so that NBI of energy as low as 30 keV is super-Alfvénic, $V_{beam}^0 > V_A$. For example, in the case of 30 keV hydrogen NBI on START,

$$V_{beam}^0 \approx 2.4 \cdot 10^6 \text{ m/s} > V_A \approx 10^6 \text{ m/s}. \qquad (10)$$

For a beam with such initial speed, the fundamental resonance, $V_{\|beam} = V_A$, is unavoidable during the beam slowing-down from V_{beam}^0 to V_{beam}. The discrete spectra of weakly-damped TAEs are usually excited at low NBI power in ST discharges.

Figure 1 shows an example of multiple discrete modes seen as peaks in the Fourier power spectrum of the perturbed poloidal magnetic field in the toroidicity-induced gap frequency range, $f_{TAE} = \omega_{TAE} / 2\pi = V_A / 4\pi q R_0 \cong$ 200-250 kHz. This spectrum of fixed-frequency TAEs was observed during the early stage of START discharge with P_{NBI} ~ 0.5 - 0.3 MW, E_0 ~ 30keV.

Similar Alfvén eigenmodes are detected on MAST, but the MAST data shows longer-lasting (duration in time > 20ms) modes. In comparison with the START data, more numerous unstable AE modes with a broader range of toroidal mode numbers were observed on MAST. The unstable modes have toroidal mode numbers $n = 1$ on START and $n = 1 \div 3$ on MAST, in agreement with the theoretical estimates of the maximum fast ion drive for TAEs, whose radial width, $\cong r_{AE} / (nq)$, is comparable to the drift orbit of the fast ion,

$\cong q\rho_{beam}$, where ρ_{beam} is the Larmor radius of beam particles at the Alfvén speed.

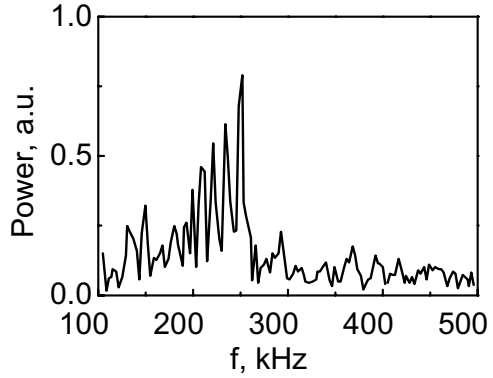

Fig. 6. Fourier power spectrum of outer midplane Mirnov coil signal $\partial\delta B_{Pol}/\partial t$ from START discharge 35305 at $t\approx$ 26 ms (β < 3%). The spectrum of TAEs is seen at $f \le 250$ kHz.

Discrete TAEs are excited most easily because they have no strong continuum damping, and their most significant damping due to the $l+1$-order side-band resonance with thermal ions of the plasma [24],

$$V_{\|i} = V_A\left(1 + l/\left(k_\| qR_0\right)\right)^{-1},\ l-\text{integer} \qquad (11)$$

is small enough at low β_i :

$$\frac{\gamma_i}{\omega} \approx -\frac{\pi^{1/2}}{4}\beta_i q^2 \Lambda\, 1\left[+\left(1+2\left(T_e/T_i\right)+2\Lambda^2\right)^2\right]\cdot e^{-\Lambda^2} \qquad (12)$$

where $\Lambda = V_A/\left(3\ V_{Ti}\right) = 1/\left(3\beta_i^{1/2}\right)$ for $l=1$, and r_{TAE} is the minor radius at which TAE is localised.

AEs driven by the radial gradient of energetic ions on STs change significantly with increasing β and for increasing beam ion energy content, β_{beam}/β. The range of β-values at which core-localised TAEs were observed in the START and MAST experiments was found to be limited to approximately $\beta \le 5\%$, although in some cases TAEs localised away from the plasma centre were seen at higher values of β. In order to investigate this β-limit for TAEs, we consider a set of tight-aspect ratio equilibria typical of START discharges at the time of the beam-driven Alfvén activity, as β increases from 4% to 6%, for a fixed value of the on-axis safety factor ($q(0) = 1.15$ was used). These equilibria are characterised by the same inverse aspect ratio $a/R_0 = 0.737$, ellipticity of the plasma cross-section ($b/a = 1.511$), and triangularity ($\delta =$ 0.34). The ideal incompressible MHD code MISHKA-1 [25] was used to compute toroidal Alfvén eigenfunctions in these equilibria. Computations using MISHKA-1 reveal two core-localised TAEs: a lower core-localised TAE with a frequency close to the bottom of the TAE-gap, and an upper core-localised TAE with a frequency close to the top of the TAE-gap. Figure 7 shows the radial structure and the eigenfrequency value λ, $\lambda \equiv \omega R_0/V_A(0)$, for the n=2 toroidal Alfvén eigenmode at increasing values of plasma β.

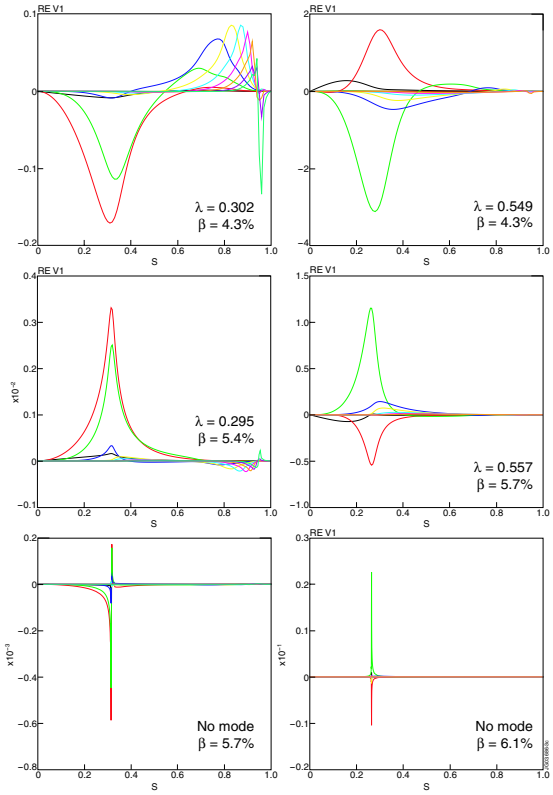

Fig. 7. The radial structure of the eigenfunctions of lower (left) and upper core-localised TAE at different values of thermal plasma β.

It is seen in Fig.7 that the radial width of both the lower- and the upper- core-localised modes shrinks with increasing plasma pressure and the mode frequencies approach the Alfvén continuum. The lower core-localised TAE coalesces with the bottom of the Alfvén continuum at around β >5.4%, while the upper core-localised TAE moves into the top Alfvén continuum at a somewhat higher β-value, β >5.7%. No core-localised TAEs were found in this type of tight-aspect-ratio equilibrium at higher values of β. Considering the equilibrium with a β-value closest to the threshold at which the TAEs disappear, β =5.4%, we find that the suppression of the core-localised TAEs by high plasma pressure is close to the well-known threshold values of the plasma pressure parameter [26]

$$\alpha = \alpha_{crit}^{\pm} = \varepsilon + 2\Delta' \mp S^2, \qquad (13)$$

where the signs + and – correspond to the upper and lower core-localised TAE, $\varepsilon = r_{TAE}/R_0$; Δ' is the Shafranov shift derivative, S is the magnetic shear, and the normalised pressure gradient is given by $\alpha = -R_0 q^2 d\beta/dr$. Thus we conclude that the experimentally observed β-threshold for

the core-localised TAE observations can be explained by the pressure effect on the existence of TAEs. The thermal ion Landau damping [24], which enhances the mode dissipation with an increase in thermal plasma β, causes a further reduction in the threshold values of β.

As β increases and TAEs disappear, the so-called "chirping" modes, which sweep down in frequency, persist up to approximately $\beta \cong 15\%$ and they become the dominant Alfvén instability for this range of β-values [27]. The chirping modes on START were observed close to the $q=3$ surface as indicated by soft X-ray diagnostics and they had mainly $n=1$, $m=3$ mode numbers. Chirping modes in START caused only a minor change in the plasma stored energy never exceeding a 3% decrease during a single burst of the mode, which would then be restored before the onset of the next pulse, so that the time-averaged evolution of the stored energy remains unaffected. Figures 8 and 9 show evolution of plasma parameters during the chirping mode activity and a magnetic spectrogram of chirping modes in this START discharge.

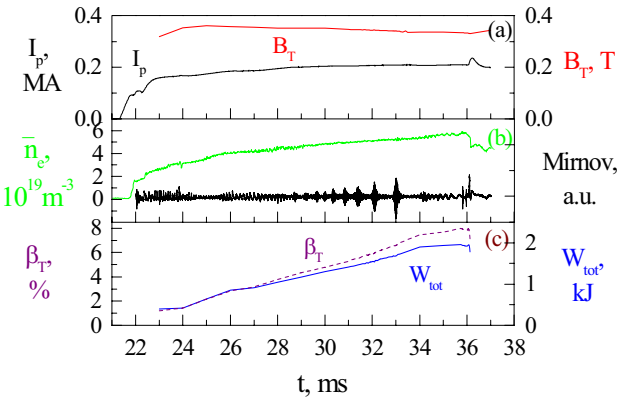

Fig.8 Evolution of plasma current I_P, toroidal magnetic field B_{or}, line-averaged plasma density, volume-averaged toroidal β, plasma energy content, and the bursts of magnetic perturbations in NBI heated START discharge #35159.

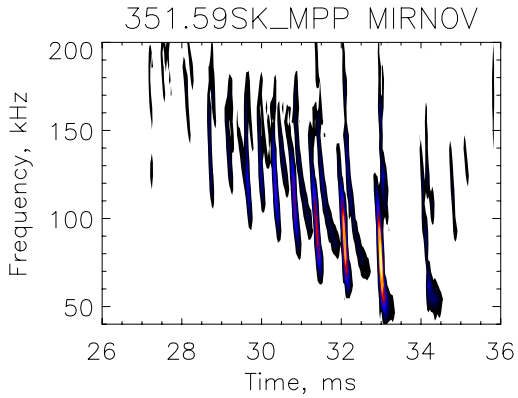

Fig.9 Magnetic spectrogram showing amplitude of chirping modes as a function of time and frequency in START discharge #35159 shown in Fig.8.

The "chirping" modes sweep in frequency by about a factor of two, and their sweeping is a linear function of time. An interpretation of these chirping modes can be given [27] in terms of EPMs [8] that can exist at high values of the beam energy content, β_{hot}/β. The fast particle contribution to the total pressure on START and MAST has been evaluated using the TRANSP code and a fast ion Monte Carlo code LOCUST. Due to the relatively low neutral beam energy (< 35 keV on START) and typically high plasma density (2 - 10x10^{19}m^{-3}), the fast ion contribution did not exceed 20% for typical medium and high-β START discharges. On MAST, with lower plasma densities and higher beam energy in high-β regimes the fast particle fraction is usually higher than on START, approaching $\beta_{hot}/\beta \approx$ 30-40% for the lowest density cases. Typically, the fast particle fraction β_{hot}/β does not increase and often decreases with increasing β.

Similar chirping modes, but over a wider range of toroidal mode numbers, are observed on MAST. Considering the β-dependence of the chirping modes, one observes a clear decrease in the amplitude of the chirping modes as the value of thermal β increases for comparable slowing-down times of the beam as shown in Figure 10.

Figure 10 presents statistics for the maximum amplitudes of chirping modes plotted as a function of β in several similar NBI discharges on MAST. A clear decrease in the amplitude with the β – value is seen, with the mode amplitudes close to zero at β=15%. Such a decrease in the chirping mode amplitude is most likely to be caused by a significant increase of the thermal ion Landau damping [24] as the value of thermal $\beta_i = (V_{Ti}/V_A)^2$ increases.

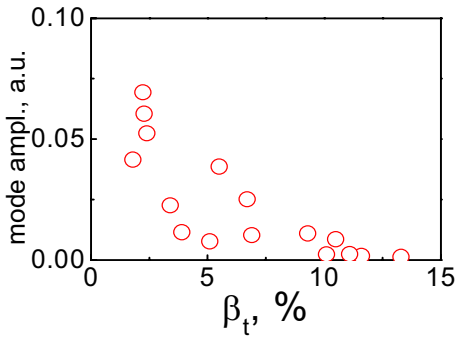

Fig.10 Dependence on β of the maximum amplitude in a single burst of chirping modes, in NBI discharges on MAST.

IV Nonlinear AE evolution

In addition to the knowledge of AE spectra, it is important to learn whether the unstable mode exhibits a soft or hard regime of nonlinear evolution. In the cases of ICRH driven TAE on JET and C-MOD, the TAE amplitude is almost always constant in time (soft regime). In this case, a saturation of the TAE instability is simply caused by flattening of the fast ion distribution function in regions of phase space that resonates with the excited TAE frequency. However, some JET discharges with ICRH and MAST discharges with NBI exhibit a more complex evolution of the

TAE-amplitudes and frequencies associated with the variety of non-linear regimes near marginal stability [28], when $\gamma_L - |\gamma_{damping}| << \gamma_L,\ |\gamma_{damping}|$.

Figure 11 shows the so-called "pitchfork splitting" of the TAE-frequency in NBI heated MAST discharge, similar to the JET experiments [29]. In this case, both TAE amplitude and fast ion pressure slowly oscillate around their saturation states. The modulation of the TAE amplitude produces the splitting of the TAE spectral line into several harmonics closely spaced in frequency.

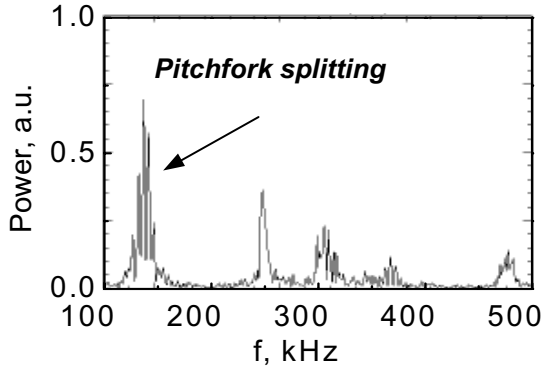

Fig. 11. Fourier power spectrum from Mirnov coil signal $\partial \delta B_{Pol} / \partial t$ for MAST discharge 2884. Pitchfork splitting of the TAE spectral line is seen at $f \leq 150$ kHz.

For a larger difference between the net drive of the TAE, $\gamma \equiv \gamma_L - |\gamma_{damping}|$, and the characteristic inverse time required for a replenishment of the distribution function, ν_{eff}, an "explosive" hard regime of TAE-amplitude has been predicted and identified on the spherical tokamak MAST. In this case, the oscillations of the beam ion pressure around the quasi-linear "plateau" are so strong, that long-living non-linear fluctuations (similar to BGK-type modes) are born. These fluctuations look like holes and clumps on the beam ion distribution function, and the frequencies of such fluctuations don't remain fixed, but sweep either up or down, with the sweeping rate depending on the mode amplitude. Figure 12 shows an example of such non-linear TAE-evolution (MAST discharge 5568) [30].

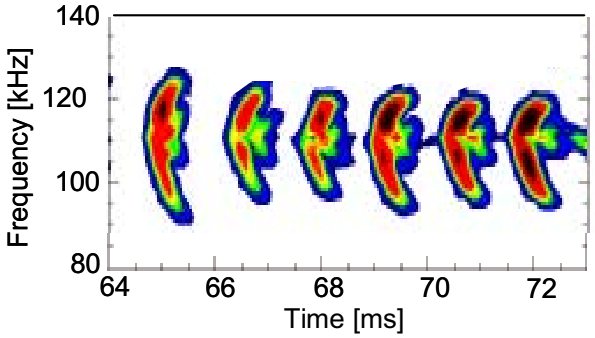

Fig. 12. Magnetic spectrogram (amplitude as function of time and frequency) of up-and-down sweeping modes in MAST.

V. Summary

In summary, one concludes that all present day machines with super-Alfvénic fast ions exhibit AE instabilities similar to the ones expected for burning plasmas. The properties of the experimentally observed AE spectra are in a broad agreement with theory of AEs. In most cases, the AE instabilities saturate at low level and do not cause significant redistribution or losses of fast ions. The low amplitude detectable AEs can be used for MHD spectroscopy.

The low toroidal magnetic field of the STs makes START and MAST a perfect test bed for studying energetic particle driven modes due to the super-Alfvénic nature of NBI at energy as low as 30 keV. Numerous Alfvén instabilities excited by NBI-produced energetic ions have been observed on START and MAST: fixed-frequency modes in the TAE and EAE frequency ranges, TAEs with the "pitchfork splitting" and with the "hole-clump" frequency-sweeping pairs of nonlinear modes, and the "chirping" modes. Data analysis shows that as β increases, the two major pressure-gradient driven fast ion instabilities, core-localised TAEs and EPM chirping modes, decrease both in mode amplitude and in the number of unstable modes.

Acknowledgements. This work was partly funded by the United Kingdom Engineering and Physical Sciences Research Council and by EURATOM. The views and opinions expressed herein do not necessarily reflect those of the European Commission.

References

(1) J.Wesson, Tokamaks, Clarendon Press, Oxford, 1987
(2) R.Aymar et al., *Plasma Phys. Control. Fusion* **44** (2002) 519
(3) A.B.Mikhailovskii 1975 *Sov. Zh.ETPh.* **41** 890
(4) G.Y. Fu and J.W. Van Dam 1989 *Phys. Fluids B* **1** 1949
(5) C.Z. Cheng, L. Chen, M.S. Chance 1985 *Ann. Phys.* **161** 21
(6) H.L. Berk *et al*., 2001 *Phys. Rev. Lett*. **87** 185002
(7) S.E. Sharapov *et al*., 2002 *Physics of Plasmas* **9** 2027
(8) L. Chen 1994 *Phys. Plasmas* **1** 1519
(9) W.W. Heidbrink et al. 1991 *Nucl. Fusion* **31** 1635
(10) L.E. Zakharov, 2004 *Fusion Eng. Design* **72** 149
(11) P.H.Rebut *et al., Proc. of 10th Intern. Conf., Plasma Physics and Controlled Nuclear Fusion, London* (International Atomic Energy Agency, Vienna, 1985), Vol.I, p.11
(12) J.A. Snipes et al., *Physics of Plasmas* **12** (2005) 056102
(13) B.Coppi et al. 2001 *Nucl. Fusion* **41** 1253
(14) D.M.Meade et al., 2001 *Proc. 18th IAEA Fusion Energy Conference, Sorrento, Italy (Vienna: IAEA)*
(15) Y-K.M. Peng and D.J. Strickler 1986 *Nucl. Fusion* **26,** 769
(16) M.P. Gryaznevich et al 1998 *Phys. Rev. Lett.* **80** 3972
(17) H.R. Wilson et. al. 2002 *Proc. 19th IAEA Fusion Energy Conference, Lyon, France, IAEA-CN-94/FT/1-5*
(18) A.Fasoli et al., 1997 *Plasma Phys. Control. Fusion* **39** B287
(19) B.N. Breizman *et al*., 2003 *Physics of Plasmas* **10** 3649
(20) P.Sandquist *et al*., 2007 *Physics of Plasmas* **14**
(21) S.E. Sharapov S.E. *et al*., 2004 *Phys. Rev. Lett.* **93** 165001
(22) S.E. Sharapov et al., 2007 *Nucl. Fusion* **47** S868
(23) M.P. Gryaznevich and S.E. Sharapov 2004 *Plasma Phys. Control. Fus.* **46** S15
(24) R. Betti and J.P. Freidberg 1991 *Phys. Fluids B* **3** 1865
(25) A.B.Mikhailovskii et al. 1997 *Plasma Phys. Reports* **23** 844
(26) H.L. Berk et al. 1995 *Phys. Plasmas* **2** 3401
(27) M.P. Gryaznevich and S.E. Sharapov 2000 *Nucl. Fusion* **40** 907
(28) H.L.Berk et al. 1998 *Phys. Lett. A* **234** 408
(29) A.Fasoli et al. 1998 *Phys. Rev. Lett.*. **81** 5564
(30) S.D.Pinches et al. 2004 *Plasma Phys. Control. Fus.* **46** S55